

Genetic deletion of the ghrelin receptor (GHSR) impairs growth and blunts endocrine response to fasting in *Ghsr-IRE5-Cre* mice



Fiona Peris-Sampedro¹, Iris Stoltenborg¹, Marie V. Le May¹, Jeffrey M. Zigman^{2,3,4}, Roger A.H. Adan^{1,5}, Suzanne L. Dickson^{1,*}

ABSTRACT

Objective: The orexigenic hormone ghrelin exerts its physiological effects by binding to and activating the growth hormone secretagogue receptor (GHSR). The recent development of a *Ghsr-IRE5-Cre* knock-in mouse line has enabled to genetically access GHSR-expressing neurons. Inserting a *Cre* construct using a knock-in strategy, even when following an upstream internal ribosome entry site (*IRE5*) can, however, interfere with expression of a targeted gene, with consequences for the phenotype emerging. This study aimed to phenotype, both physically and metabolically, heterozygous and homozygous *Ghsr-IRE5-Cre* mice, with a view to discovering the extent to which the ghrelin signalling system remains functional in these mice.

Methods: We assessed feeding and arcuate nucleus (Arc) Fos activation in wild-type, heterozygous and homozygous *Ghsr-IRE5-Cre* mice in response to peripherally-administered ghrelin. We also characterised their developmental and growth phenotypes, as well as their metabolic responses upon an overnight fast.

Results: Insertion of the *IRE5-Cre* cassette into the 3'-untranslated region of the *Ghsr* gene led to a gene-dosage GHSR depletion in the Arc. Whereas heterozygotes remained ghrelin-responsive and more closely resembled wild-types, ghrelin had reduced orexigenic efficacy and failed to induce Arc Fos expression in homozygous littermates. Homozygotes had a lower body weight accompanied by a shorter body length, less fat tissue content, altered bone parameters, and lower insulin-like growth factor-1 levels compared to wild-type and heterozygous littermates. Moreover, both heterozygous and homozygous *Ghsr-IRE5-Cre* mice lacked the usual fasting-induced rise in growth hormone (GH) and displayed an exaggerated drop in blood glucose and insulin compared to wild-types. Unexpectedly, fasting acyl-ghrelin levels were allele-dependently increased.

Conclusions: Our data suggest that (i) heterozygous but not homozygous *Ghsr-IRE5-Cre* mice retain the usual responsiveness to administered ghrelin, (ii) the impact of fasting on GH release and glucose homeostasis is altered even when only one copy of the *Ghsr* gene is non-functional (as in heterozygous *Ghsr-IRE5-Cre* mice) and (iii) homozygous *Ghsr-IRE5-Cre* mice exhibit growth retardation. Of the many transgenic models of suppressed ghrelin signalling, *Ghsr-IRE5-Cre* mice emerge as best representing the full breadth of the expected phenotype with respect to body weight, growth, and metabolic parameters.

© 2021 The Author(s). Published by Elsevier GmbH. This is an open access article under the CC BY-NC-ND license (<http://creativecommons.org/licenses/by-nc-nd/4.0/>).

Keywords Ghrelin; *Ghsr-IRE5-Cre* mice; Growth; Growth hormone; IGF-1; Arcuate nucleus

1. INTRODUCTION

The stomach-derived hormone ghrelin is secreted pre-prandially and conveys hunger information to the brain by acting via the growth hormone secretagogue receptor (GHSR, ghrelin receptor) [1–3]. Besides being powerfully orexigenic [4,5], ghrelin is also key for signalling other aspects of negative energy balance; it exerts glucoregulatory actions that are crucial for survival upon life-threatening conditions [6], and promotes weight gain and adiposity

[7]. Apart from contributing to these homeostatic functions, and its initially described role in stimulating growth hormone (GH) release from the pituitary [3], the ghrelin system is likewise implicated in the stimulation of hedonic aspects of feeding [8–11]. Thus, GHSR is expressed in brain regions important for energy homeostasis and also in those linked to reward, learning, and memory. These include the hypothalamic arcuate nucleus (Arc), together with other mediobasal hypothalamic (MBH) nuclei, as well as the ventral tegmental area (VTA), amygdala, hippocampus, nucleus accumbens and various

¹Department of Physiology/Endocrinology, Institute of Neuroscience and Physiology, The Sahlgrenska Academy at the University of Gothenburg, Gothenburg, Sweden ²Center for Hypothalamic Research, Department of Internal Medicine, UT Southwestern Medical Center, Dallas, TX, USA ³Division of Endocrinology, Department of Internal Medicine, UT Southwestern Medical Center, Dallas, TX, USA ⁴Department of Psychiatry, UT Southwestern Medical Center, Dallas, TX, USA ⁵Department of Translational Neuroscience, UMC Utrecht Brain Center, Utrecht University, Utrecht, The Netherlands

*Corresponding author. Department of Physiology/Endocrine, Institute of Neuroscience and Physiology, The Sahlgrenska Academy at the University of Gothenburg, Medicinaregatan 11, SE405 30, Gothenburg, Sweden. E-mail: suzanne.dickson@neuro.gu.se (S.L. Dickson).

Received February 26, 2021 • Revision received March 22, 2021 • Accepted March 24, 2021 • Available online 31 March 2021

<https://doi.org/10.1016/j.molmet.2021.101223>

brainstem areas, including the lateral parabrachial nucleus (IPBN) [12–14].

Over the past 15 years, numerous loss-of-function studies in mice that lack components of the ghrelin system have contributed to enhance our understanding on the physiological role of the hormone; however, they have led to conflicting results [15–21]. For example, some of the initial targeted-deletion studies did not find blunting GHSR function to cause a reduction in body weight and/or adiposity [19,20], whereas others indicated the establishment of a leaner phenotype as a consequence of this genetic manipulation [15–17,21]. This leaner phenotype has been attributed to enhanced insulin sensitivity, elevated energy expenditure, higher resting metabolic rate, decreased food intake, and/or reduced respiratory quotient, among other factors [15,16,21]. Given the documented effects of ghrelin and ghrelin mimetics on GH secretion, it is surprising that none of the aforementioned studies, with the exception of [21], considered that disrupting ghrelin signalling may affect one or more components of the GH-growth axis, which could also contribute to a leaner phenotype.

The Cre-LoxP system [22] has permitted studying gene function *in vivo* by introducing desired conditional targeted mutations into the mouse genome. Technical advances mitigating off-target effects have led to new *Cre*-lines whereby *Cre* expression is directed, endogenously, by the promoter of a gene of interest [23]. The development of the first *Ghsr-IRES-Cre* model [12] offers the possibility to manipulate and control specific subsets of GHSR-expressing neurons, and thus stands as a valuable tool to explore and control the ghrelin-responsive neuronal circuitry. In this mouse line, an *IRES-Cre-FRT-neo-FRT* cassette (*IRES*: internal ribosomal entry site; *FRT*: flipase recombination target; *neo*: neomycin resistant gene) is knocked-in to the 3'-untranslated region (-UTR) of the murine *Ghsr* gene. The pattern of GHSR distribution in heterozygous *Ghsr-IRES-Cre* mice faithfully mirrored that previously observed [14]. It has been suggested, however, that inserting a *Cre* construct into the 3'-UTR can interfere with expression of the targeted gene in a gene-dosage fashion, with consequences on the emergence of the phenotype [24–27]. This disruption can occur despite the addition of the *IRES* cassette, which theoretically should permit synthesis of both GHSR and *Cre* recombinase from the modified *Ghsr* locus.

In the present study, we sought to phenotype both heterozygous and homozygous mutants, in terms of their ghrelin-responsivity (by exploring administered ghrelin-induced food intake and Fos protein expression in the Arc), their metabolic response upon an overnight fast and their growth progression. Based on our somewhat unexpected observation that homozygous *Ghsr-IRES-Cre* mice appeared to have a lower body weight, we reasoned that GHSR signalling may be disrupted in these mice and that this could have consequences for the aforementioned metabolic and growth traits.

2. MATERIALS AND METHODS

2.1. Mice

We used the same strain of *Ghsr-IRES-Cre* mice as previously described [12]. Heterozygous *Ghsr-IRES-Cre* mice that had already been backcrossed several generations onto a C57BL/6N in Dallas, TX and then Melbourne, AU were subsequently backcrossed to C57BL/6N (Charles River, Sulzfeld, Germany; strain code: 027) another six generations. From the resulting offspring, heterozygous mice were selected as breeders to generate the mice used in our study. Pregnant females were examined daily, and the day of delivery was designated as postnatal day (PND) 0. Genotyping of the offspring was carried out on PND 12 as described previously [12]. After weaning on PND 28,

mice were group-housed (2–5 mice per cage) and left undisturbed until the beginning of the experimental procedures, except for experiment 3 in which mice were tested from PND 12. Each experimental group consisted of offspring from at least four different litters, unless otherwise stated, and only male mice were used.

Mice were kept on a 12-h dark–light cycle (lights off: 7 pm) at 20–22 °C and 50% humidity and had always free access to water and standard maintenance chow (2018 Teklad global 18% protein rodent diet, Envigo, Somerset, NJ, US), unless otherwise stated. All experiments were approved by the local ethics committee for animal care in Gothenburg, Sweden (Göteborgs djurförsöksetiska nämnd; permits number 132–2016 and 3112–2020) and complied with European guidelines (Decree 86/609/EEC).

2.2. Experiment 1: *Ghsr* mRNA detection by RNAscope in the arcuate nucleus of wild-type, heterozygous and homozygous *Ghsr-IRES-Cre* mice

Adult wild-type ($n = 4$), heterozygous ($n = 4$), and homozygous ($n = 4$) *Ghsr-IRES-Cre* mice were used to explore GHSR expression in the arcuate nucleus (Arc), a key MBH site normally expressing high levels of GHSR [12–14]. To that end, fluorescent *in situ* hybridisation using RNAscope® was performed according to published protocols [28].

Mice were deeply anaesthetised with a mixture of Sedastart vet.® (1 mg/kg; Produlab Pharma B.V., Raamsdonksveer, The Netherlands) and Ketalar® (75 mg/kg; Pfizer AB, New York, NY, USA) [28], prior to being perfused transcardially with heparinized 0.9% saline followed by 4% paraformaldehyde (PFA) in 0.1 M phosphate buffer (PB). The brains were quickly removed, stored overnight at 4 °C in a 4% PFA fixative solution, and cryoprotected in 0.1 M PB containing 25% sucrose at 4 °C until cryosection. Coronal sections containing the Arc (14- μ m-thick, every 6th section collected to provide 6 adjacent series) were cut using a cryostat and stored in an antifreeze solution (25% glycerine, 25% ethylene glycol, and 50% 0.1 M autoclaved PB) at –20 °C until further processing.

All reagents were purchased from Advanced Cell Diagnostics (ACD, Hayward, CA, USA), unless otherwise stated. The *Ghsr* probe (#426141-C3) contained 20 oligonucleotide pairs and targeted region 438–1385 (Acc. No. NM_177330.4) of the *Ghsr* transcript. Negative and positive control probes recognizing bacterial dihydrodipicolinate reductase, DapB (#320871) and PolR2A, cyclophilin and Ubiquitin (#320881) were processed in parallel with the target probe to ensure RNA integrity and an optimal assay performance. All incubation steps were performed at 40 °C using a humidified chamber and a HybEZ oven (#321462). On the day before the assay, the sections were mounted onto SuperFrost Plus slides (#631-9483; VWR, Radnor, PA, USA), dried at room temperature, briefly rinsed in autoclaved Milli-Q purified water, air-dried and baked at 60 °C overnight. On the day of the assay, slides were first incubated for 7 min in hydrogen peroxide (#322335), submerged in Target Retrieval buffer (#322001) at a temperature of 98 °C for 7 min, followed by 2 brief rinses in autoclaved Milli-Q purified water. The slides were quickly dehydrated in 100% ethanol and allowed to air-dry for 5 min. All the sections were incubated with Protease Plus (#322331) for 30 min. The subsequent steps (i.e., hybridisation of the probes and the amplification and detection steps) were performed according to the manufacturer's protocol for the tyramide-based RNAscope® Multiplex Fluorescent v2 Assay (#323100). For detection of the probe directed towards *Ghsr* mRNA, a Cy5 tyramide (1:2000; Akoya Biosciences, Menlo Park, CA, USA) was used. All the sections were counterstained with DAPI, coverslipped with ProLong® Diamond Antifade mountant (#P36970; Thermo Fisher

Scientific, Waltham, MA, USA) and stored in the dark at 4 °C until imaging.

Images for the quantification of RNAscope data were captured using a laser scanning confocal microscope (LSM 700 inverted, Zeiss, Oberkochen, Germany) equipped with a Plan-Apochromat 40x/1.3 Oil DIC objective (used at the Centre for Cellular Imaging at Gothenburg University). Tile scans (4 × 4) and Z-stacks (optical section of 1.0 μm) of the Arc-containing sections were captured unilaterally from rostral to caudal (3 sections per mouse at these approximate levels: 1.43, 1.67, and 1.91 caudal to Bregma). Laser intensities for the different channels were kept constant throughout the imaging process. The Z-stack images were processed using the maximum intensity projection function in the Zen Black software (Zeiss). The final images were then stitched, the channels were merged and the cells manually counted in ImageJ/Fiji (NIH, Bethesda, MD, USA) using the Cell counter plug-in. DAPI stain was used for cellular recognition. DAPI-identified cells with >1–3 dots/cell were defined as being *Ghsr*-positive. The mean number of *Ghsr*-positive cells per hemisection (and averaged per three blind countings) was calculated, then averaged for each brain and ultimately for each experimental group. Of note, the counting did not contemplate a scoring system, and thus was irrespective of the quantity of dots a given *Ghsr*-expressing cell had above the 1–3 dots/cell threshold.

2.3. Experiment 2: assessment of ghrelin-responsiveness in wild-type, heterozygous and homozygous *Ghsr-Cre* mice

2.3.1. Body weight and food intake under ad libitum condition

Mice were first allowed to acclimate to single housing for a week. To simplify the search for food pieces during measurements, the mice were habituated to a new environment in which the bedding was replaced with tissue paper (to retain comfort and environmental enrichment) [29]. They were provided with ad libitum access to water and regular chow on the cage floor. Both body weight and daily food intake were monitored regularly, at the same time of the day, prior to ghrelin administration. Body weight was measured again prior to sacrificing the mice (i.e., 2 weeks after ghrelin injection).

2.3.2. Administered ghrelin-induced food intake

Ghrelin-induced food intake was assessed in adult wild-type (n = 9), heterozygous (n = 9), and homozygous (n = 6) *Ghsr-IRES-Cre* mice. Mice received subcutaneous (s.c.) injections of saline for three consecutive days for habituation to the procedure. Injections were performed in a cross-over fashion: every animal at one point received either ghrelin or an equal volume saline vehicle one day apart. On the experimental day, food was withdrawn from the cages during the light period (9 am) for 3 h, after which ghrelin (3 mg/kg BW s.c.; #1465; Tocris, Bristol, UK) or saline was administered. Immediately after injection, pre-weighed regular chow was re-introduced on the cage floor. Food intake was manually measured at 3 and 24 h post-ghrelin administration using calibrated scales that had a precision of 1 mg. Mice were also weighed 24 h post-ghrelin administration in order to determine the transient impact of peripherally administered ghrelin on weight gain.

2.3.3. Administered ghrelin-induced Fos protein expression

Ghrelin-induced Fos protein expression in the Arc was counted in adult wild-type (n = 11), heterozygous (n = 12), and homozygous (n = 10) *Ghsr-IRES-Cre* mice. Body weight-matched mice from the 3 genotypes were allocated into 2 groups: a vehicle group (Wt, n = 3; Het, n = 4; and Hom, n = 3), which received an s.c. injection of saline and a

ghrelin group (Wt, n = 8; Het, n = 8; and Hom, n = 7), which received a 3 mg/kg body weight s.c. injection of ghrelin instead. Prior to the testing day, all mice were familiarized with the procedure. The injections were performed during the light phase (10 am–2 pm) and groups counterbalanced with respect to time of the day. The mice were perfused 90 min post-ghrelin administration, and the intake of food corresponding to that period measured. Mice were deeply anaesthetised with the mixture of Sedastart vet.® and Ketalar® mentioned above and perfused transcardially as previously described. After harvesting, the brains were stored overnight at 4 °C in a 4% PFA fixative solution containing 15% sucrose, and cryoprotected in 0.1 M PB containing 30% sucrose at 4 °C until cryosection. Coronal sections containing the Arc (30 μm thickness) were cut using a cryostat and stored in an antifreeze solution (25% glycerine, 25% ethylene glycol, and 50% 0.1 M PB) at –20 °C until further processing.

Free-floating sections were processed for the immunohistochemical detection of Fos protein using the 3,3'-diaminobenzidine (DAB)-hydrogen peroxidase method [30]. Briefly, after deactivation of endogenous peroxidases, the sections were rinsed with 0.1 M PB + 0.3% Triton X-100 before being blocked for 1 h at room temperature in 0.1 M PB, 3% normal goat serum, 0.25% bovine serum albumin, and 0.3% Triton X-100. They were then incubated with an anti-c-Fos rabbit primary antibody (dilution 1:20 000; Ab-5 (4–17) Rabbit pAb, PC38; Calbiochem, San Diego, CA, USA) over three nights. Subsequently, the sections were rinsed and incubated for 2 h with a peroxidase goat anti-rabbit immunoglobulin (IgG) secondary antibody (dilution 1:200; PI1000; Vector Laboratories, Burlingame, CA, USA) and a DAB, nickel, and hydrogen peroxide solution. Brain sections were mounted onto glass slides and coverslipped with ProLong® Diamond Antifade mountant (Thermo Fisher).

Unilateral images of Arc-containing sections (3 sections per mouse at these approximate levels: 1.43, 1.79 and 1.91 caudal to Bregma) were acquired from rostral to caudal using a DMRB fluorescence microscope (Leica Microsystems, Wetzlar, Germany). The number of Fos-positive nuclei per brain section was counted manually in ImageJ/Fiji (NIH) as described above. The mean number of Fos-like immunoreactive nuclei per hemisection (and averaged per 3 blind countings) was calculated, averaged for each brain and ultimately for each experimental group.

2.4. Experiment 3: physical and motor development in wild-type, heterozygous and homozygous *Ghsr-IRES-Cre* mice

We sought to further explore our observation that homozygous mice had a lighter body weight than both wild-type and heterozygous peers, with a view to discard any potential severe developmental abnormality. Physical development and critical motor milestones were monitored during the early postnatal period (PND 12 to 16), locomotor activity was assessed during mid-adolescence (PND 42) and body weight progression was followed throughout the early postnatal period, adolescence and adulthood in wild-type (n = 8), heterozygous (n = 11), and homozygous (n = 8) *Ghsr-IRES-Cre* mice (Table 1). Each experimental group consisted of offspring from seven different, but quasi-simultaneous, litters from seven different breeding pairs. Screening was performed under blinded conditions.

2.4.1. Physical development and developmental motor milestones

The observational tests were adapted from a previous study [31,32]. As a measure of physical development, the pups' body weights were recorded on PND 12, 14, and 16, and eye opening from PND 12 to 16 was evaluated and scored as follows: 0 = both eyes closed; 1 = first eye opened; 2 = both eyes are clearly open. Regarding motor

Table 1 — Assessment of the physical and motor development, as well as physical endpoints, in *Ghsr-IRES-Cre* wild-type, heterozygous, and homozygous littermates.

Endpoint	Test	Day of evaluation (PND)	Measure/score
Physical development	Body weight	12, 14, 16, 28, 42, 52, 65, 66	Weight (g)
	Eye opening	12, 14, 16	0 = both eyes closed; 1 = first eye opened; and 2 = both eyes are clearly open
	Locomotor activity	42	Horizontal activity (lower beam break), locomotion (new lower beam break), and rearing activity (upper beam break) in an open field
Developmental motor milestones	Tail pull reflex	12, 14, 16	0 = the pup offers no resistance; 1 = the pup grasps the grid and offers some resistance; and 2 = the pup grasps the grid and offers strong resistance during the whole pull (4 s).
	Cling ability	12, 14, 16	0 = the pup falls off immediately; 1 = the pup falls off within 15 s; and 2 = the pup holds on for 15 s at the same position and/or starts to climb.
	Climb ability	12, 14, 16	0 = the pup falls off immediately; 1 = the pup climbs half of the grid; and 2 = the pup climbs to the top of the grid.
Physical endpoints	Body length	65	Nose-to-anus length (mm) using a digital calliper
	Body composition	65	Fat (g), lean (g), and soft tissues mass (g), bone area (cm ²), bone mineral content (BMC, mg), and density (BMD, mg/cm ²) by dual-energy X-ray absorptiometry (DXA)
	Body mass index (BMI)	65	BMI = body weight (g)/[nose-to-anus length (cm)] ²
	Body weight (after fasting)	66	Weight (g) after an overnight fast
	Femur length	66	Femur length (mm) using a digital calliper

maturation, the tail pull reflex, as well as the abilities to cling and climb were evaluated on PND 12, 14, and 16 using a metallic grid inclined at a 45° angle. A soft surface was placed underneath the grill to cushion a potential fall. The pups were first placed near the top of the grid and gently pulled backwards by the tail. The resistance offered by the pup during the pull (tail pull reflex) was recorded as follows: 0 = the pup offers no resistance; 1 = the pup grasps the grid and offers some resistance; 2 = the pup grasps the grid and offers strong resistance during the whole pull (4 s). The ability to remain on the grid (cling test) was scored as follows: 0 = the pup falls off immediately; 1 = the pup falls off within 15 s; and 2 = the pup holds on for 15 s at the same position or starts to climb. The ability to climb the grid was scored as follows: 0 = the pup falls off immediately; 1 = the pup climbs half of the grid; and 2 = the pup climbs to the top of the grid. Body weight was measured at various time points between the ages of 28–65 days (Table 1).

2.4.2. Locomotor activity in an open field

The open field boxes consisted of four different ceiling-closed 500 × 500 mm arenas (lit from above: ~150 lux), protected with 225 mm-high walls, placed inside ventilated sound-attenuated cubicles (Open field activity system, Kungsbacka Mät & Reglerteknik KRM AB, Fjärås, Sweden). Each mouse (42-day-old) was initially placed in the middle of the field and allowed to freely explore the apparatus for 60 min. The locomotor activity was recorded by an automated system using infrared beams in the X-, Y-, and Z-plane. We measured the horizontal activity (increased by one every time the animal broke a beam in the lower plane), total locomotion (increased by one every time the animal made a real locomotion; i.e., when a new beam was broken) and rearing activity (increased by one every time the animal broke a beam in the upper plane). To prevent the use of olfactory cues, we cleaned the behavioural equipment with 70% ethanol between each session.

2.5. Experiment 4: body composition, physical endpoints, and metabolic parameters in wild-type, heterozygous and homozygous *Ghsr-IRES-Cre* mice

2.5.1. Dual-energy X-Ray absorptiometry (DXA)

To further characterize the mice, both physically and metabolically, we performed dual-energy X-ray absorptiometry (DXA) to examine body

composition during adulthood (PND 65) in the same cohort of wild-type (n = 8), heterozygous (n = 11), and homozygous (n = 8) *Ghsr-IRES-Cre* mice. Under anaesthesia (mixture of Sedastart vet.® and Ketalar®), nose-to-anus body lengths were measured using a digital calliper. Tail blood was then collected (for later leptin assay) by tail bleed into EDTA-coated tubes prior to introducing the mice into the DXA chamber (Faxitron UltraFocus dual-energy X-ray absorptiometry; Faxitron Bioptics, Tuscon, AZ, USA). The parameters analysed included the following: soft tissue (i.e., all the tissue in the body that is not hardened by the processes of ossification or calcification), lean tissue, and fat tissue mass; and bone area (i.e., the total bone surface), bone mineral content (BMC), and bone mineral density (BMD). The area of analysis encompassed the head, the body trunk and the extremities, up to the third vertebra of the tail. Body mass indexes (BMI) were also calculated as follows: BMI = body weight (g)/[nose-to-anus length (cm)]². After the procedure, mice received an s.c. injection of the sedation-reversing Sedastop vet. ® (2.5 mg/kg s.c.; Produlab Pharma B.V.) [28].

2.5.2. Fasting-induced hormones levels

Wild-type (n = 8), heterozygous (n = 11) and homozygous (n = 8) *Ghsr-IRES-Cre* mice were eventually subjected to an overnight fast (~14 h) to study fasting-induced serum levels of GH, Insulin-like growth factor (IGF)-1, acyl-ghrelin, and insulin. First, fasting blood glucose was determined from tail nicks using a glucometer (Accu-Check Performa, Roche Diagnostics Scandinavia AB, Bromma, Sweden), after which the mice were weighed and deeply anaesthetised as described above. Blood was collected by cardiac puncture into clot-activator serum tubes and mice terminated by cervical dislocation. Femurs were extracted and measured using callipers.

2.5.3. Hormones analyses

For serum acyl-ghrelin levels, 4-(2-aminoethyl)benzenesulfonyl fluoride hydrochloride (AEBSF) was added (final concentration 1 mg/mL) to the collected blood. We did not acidify the sample because it has been shown that HCl addition to AEBSF-treated samples does not provide enhanced hormone stability [33]. No further processing of either the EDTA-treated or the serum intended blood was performed prior to leptin, GH, IGF-1, or insulin determinations. In general, tubes were centrifuged to obtain either plasma or serum, which were then aliquoted and stored at -80 °C until processing. Leptin (#EZML-82K;

Merck Millipore, Darmstadt, Germany), GH (#EZRMGH-45K; Merck Millipore), IGF-1 (#80574; Crystal Chem, Zaandam, The Netherlands), active ghrelin (#EZRGRA-90K; Merck Millipore), and insulin (#EZRMI-13K; Merck Millipore) levels were measured using commercial ELISA kits following the manufacturer's instructions. Samples were thawed only once.

2.6. Statistics

The program IBM SPSS Statistics 27 (IBM Corp., Armonk, NY, USA) was used for all statistical analyses. In experiment 1, we used a one-way ANOVA to assess the effects of genotype on Arc *Ghsr* expression (Figure 1). In experiment 2, food intake, body weight and weight gain were subjected to one-way ANOVA analyses (Genotype) (Figure 2). Comparisons were carried out by one-way repeated measures ANOVA (RMANOVA) when assessing the acute food intake responses and body weight change upon ghrelin administration (with genotype as “between factor” and treatment as “within factor” variables) (Figure 3). When applicable, additional RMANOVAs, with the data split according to genotype, were run as a follow-up to evaluate the differences between the saline and the ghrelin condition. Fos protein expression and 90-min food intake data were subjected to two-way ANOVA analyses (Genotype, Treatment) (Figure 4). In experiment 3, we performed one-way RMANOVA analyses (with genotype as “between factor” and time

as “within factor” variables) to study both the body weight progression throughout lifetime and the physical development and developmental motor milestones from PND 12 to PND 16 (Figure 5). In experiments 3 and 4, one-way ANOVA analyses were performed when assessing the effects of genotype on all other parameters (Figures 5 and 6, Table 2). In general, one-way ANOVA tests (and subsequent Tukey's post-hoc multiple comparisons analyses when applicable) were used to follow up significances and interactions upon split data from the three genotypes and/or ghrelin treatment.

Outliers, if any, were detected by the Grubbs' outlier test and excluded from the specific analysis. Data are expressed as mean \pm standard error of the mean. Statistical significance was set at $p < 0.05$, and values $0.05 \leq p < 0.1$ were considered evidence of statistical trends. Statistics details of the main analysis include the p value and its corresponding F ratio (together with the degrees of freedom of the numerator and denominator used to calculate it).

3. RESULTS

3.1. Homozygous *Ghsr-IRES-Cre* mice do not express *Ghsr* mRNA in the arcuate nucleus

Ghsr transcripts were barely detectable in the otherwise GHSR-abundant hypothalamic nucleus, namely the Arc, of homozygous

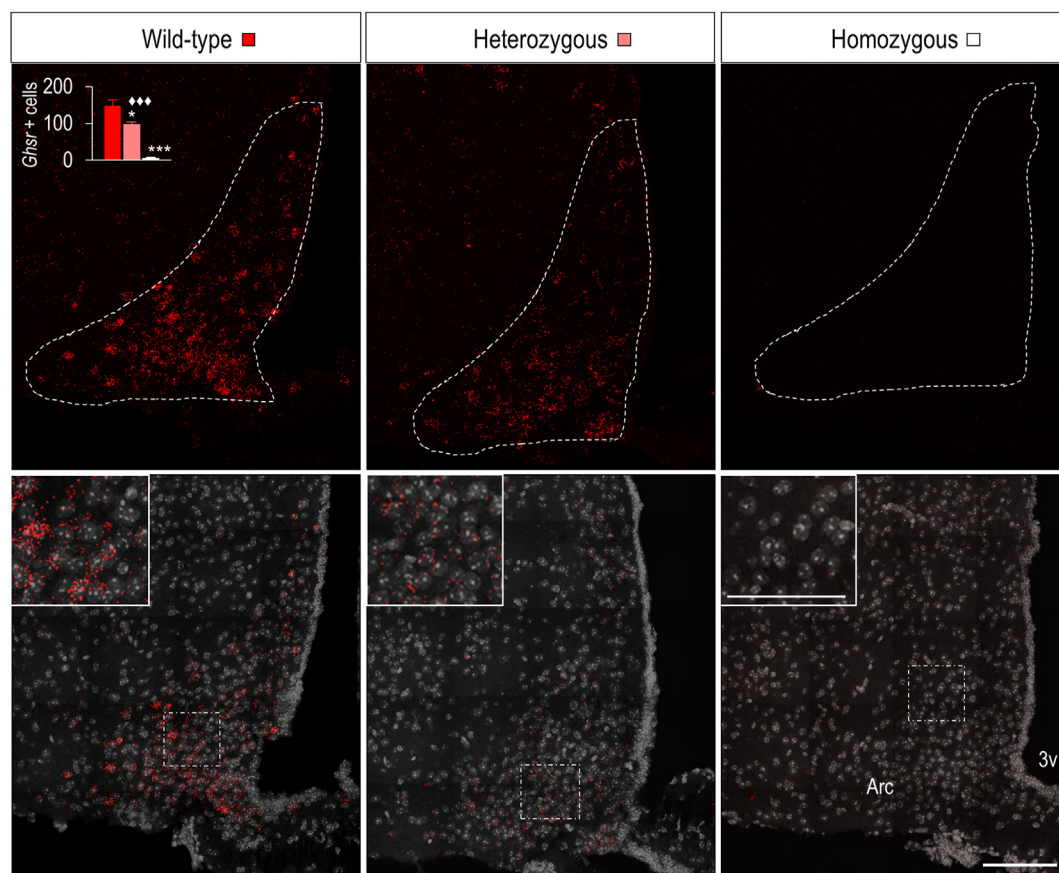


Figure 1: Expression of *Ghsr* mRNA in the arcuate nucleus of adult wild-type, heterozygous and homozygous *Ghsr-IRES-Cre* mice. Representative images of RNAscope (and magnifications of the indicated parts) for *Ghsr* mRNA (red) in the arcuate nucleus performed in wild-type, heterozygous and homozygous *Ghsr-IRES-Cre* mice. DAPI is depicted in grey. The graphic illustrates the quantification of *Ghsr*-positive (+) cells in the arcuate nucleus in wild-types (red), heterozygotes (light red) and homozygotes (white). Symbols indicate significant differences: vs. wild-types at $*p < 0.05$ or $***p < 0.001$; vs. heterozygotes and homozygotes at $\blacklozenge \blacklozenge \blacklozenge p < 0.001$. Arc, arcuate nucleus; 3V, third ventricle. Bregma: ~ -1.91 mm; scale bar = 200 μ m (applies to all 6 panels).

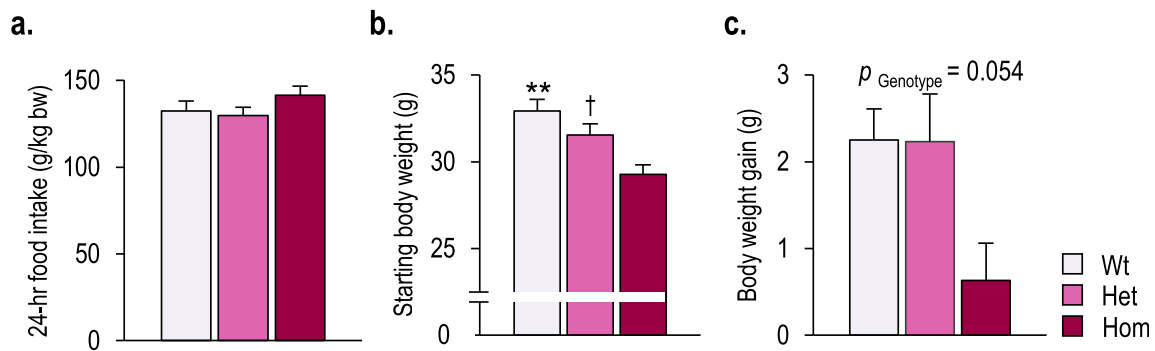


Figure 2: Food intake, body weight and body weight gain of adult wild-type, heterozygous, and homozygous *Ghnr-IRES-Cre* mice under *ad libitum* conditions. (A) Daily food intake (in g/kg body weight, bw), (B) body weight and (C) body weight gain of adult mice prior to ghrelin injection (n = 6–9/group). Symbols indicate significant differences: vs. the homozygous littermates at ** $p \leq 0.01$ or † $0.05 \leq p < 0.1$.

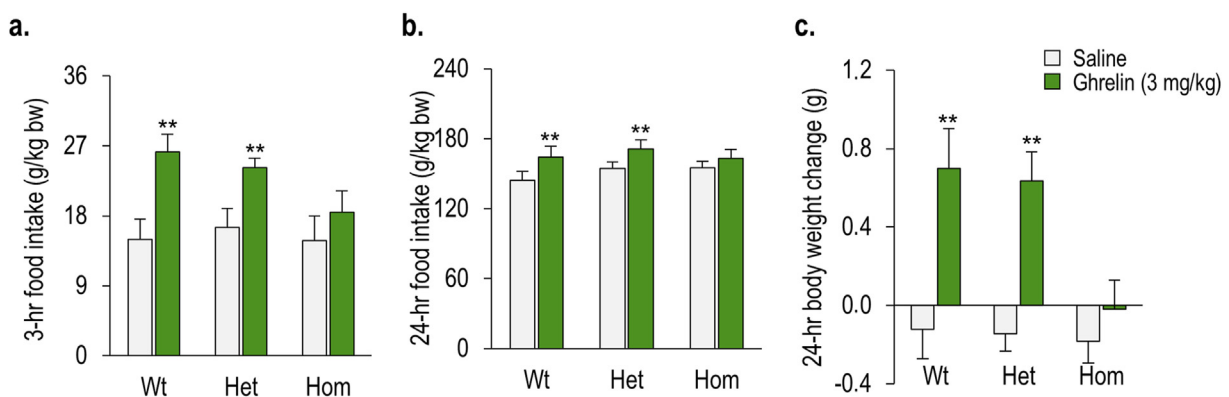


Figure 3: Orexigenic effects of peripheral ghrelin in adult wild-type, heterozygous, and homozygous *Ghnr-IRES-Cre* mice. (A) Ghrelin-induced 3 h and (B) 24 h food intake (in g/kg body weight, bw) in adult mice (n = 6–9/group). (C) Acute (24 h) ghrelin-induced body weight change in adult mice (n = 6–9/group). Symbols indicate significant differences vs. the saline condition at ** $p \leq 0.01$.

Ghnr-IRES-Cre mice, in contrast with the high levels of *Ghnr* expression observed notably in wild-type littermates (Figure 1). Strikingly, after counting *Ghnr*-positive cells, we found that this number followed a gene-dosage effect (Genotype: $F_{(2,11)} = 53.684$, $p < 0.001$). The wild-types exhibited the highest number of *Ghnr*-positive cells (147.8 ± 15.6 *Ghnr*-positive cells; wild-type vs. heterozygous, 34.0% reduction, $p = 0.013$; wild-type vs. homozygous, 95.7% reduction, $p < 0.001$), followed by the heterozygotes (97.5 ± 6.6 ; heterozygous vs. homozygous, 93.4% reduction, $p < 0.001$), whose number of cells expressing *Ghnr* was conspicuously affected by the genetic manipulation, and lastly the homozygotes (6.4 ± 0.7).

Although we carefully explored other GHSR-rich brain areas with the same attention to detail as performed for the Arc, we were unable to detect more than a very few scattered GHSR-positive cells in homozygous mice (data not shown). Importantly, we also did not detect *Ghnr* transcripts in the VTA or in the IPBN in homozygous mutants, areas where GHSR is otherwise abundant [12,14] (data not shown).

3.2. Ghrelin does not stimulate food intake or induce Arc Fos protein expression in homozygous *Ghnr-IRES-Cre* mice

We monitored body weights and food intake of individually-housed adult mice before administering ghrelin. No genotype-dependent

differences in daily food intake were observed prior to starting the experimental procedures (Figure 2A). However, starting body weights did differ between genotypes (Genotype: $F_{(2,23)} = 7.367$, $p = 0.004$). Specifically, adult homozygous mice were lighter than both wild-type ($p = 0.003$) and heterozygous ($p = 0.066$) littermates before the administration of ghrelin (Figure 2B). Body weight following the ghrelin vs. saline crossover study (see below) was measured again prior to sacrificing the mice. Interestingly, the weight gain in homozygous mice was essentially nil, unlike that of both wild-type and heterozygous littermates, which increased expectedly and to the same degree (Genotype: $F_{(2,23)} = 3.365$, $p = 0.054$) (Figure 2C).

Prior to their sacrifice, these mice were subjected to a cross-over experimental design, in which they received a peripheral injection of either ghrelin or saline, after which we determined the impact on food intake. The statistic output revealed a robust overall effect of the treatment for each of the time points studied (Treatment: 3 h, $F_{(1,23)} = 20.542$, $p < 0.001$; and 24 h, $F_{(1,23)} = 21.116$, $p < 0.001$). We found that, importantly, ghrelin did not stimulate food intake in homozygous *Ghnr-IRES-Cre* mice as it did in their wild-type and heterozygous littermates (Figure 3). Specifically, ghrelin increased 3 and 24 h food intake over that induced by saline in wild-type (3 h,

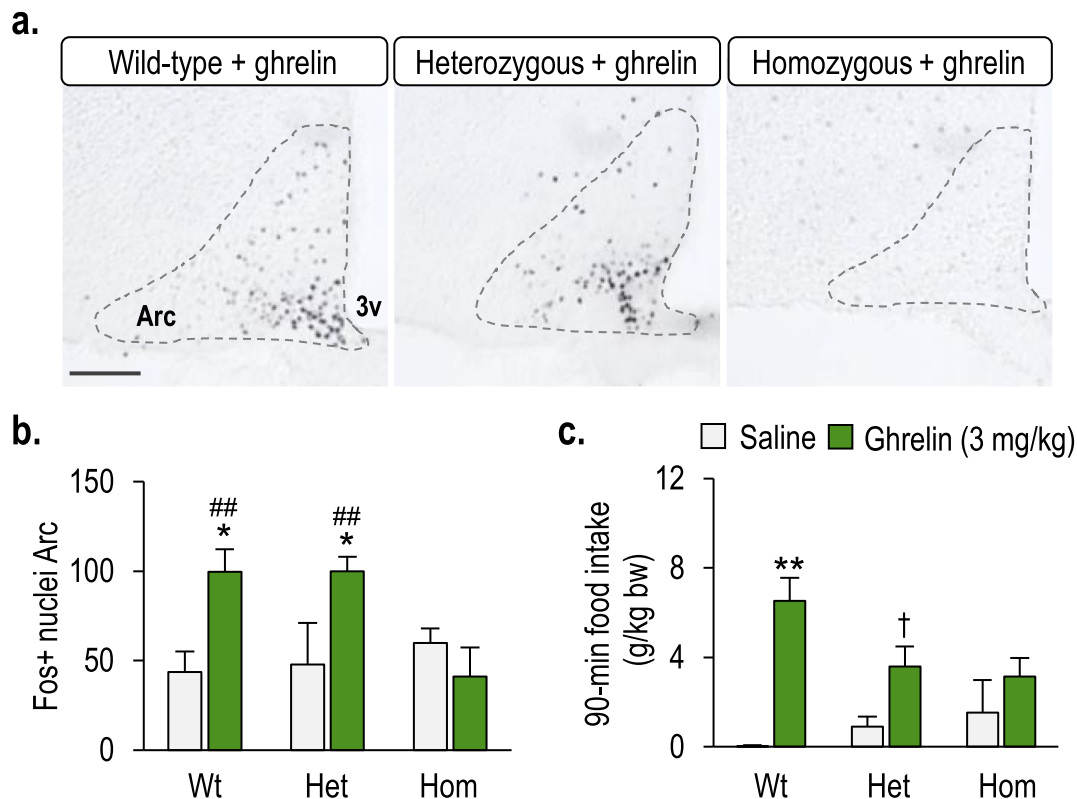


Figure 4: Ghrelin-induced Fos protein expression in the arcuate nucleus of adult wild-type, heterozygous, and homozygous *Ghnr-IRES-Cre* mice. (A) Representative images showing effects of ghrelin to increase the number of cells detected that express Fos-protein, revealed by immunohistochemistry, in the arcuate nucleus of wild-type, heterozygous and homozygous *Ghnr-IRES-Cre* mice. Arc, arcuate nucleus; 3V, third ventricle. Bregma: ~ -1.91 mm; Scale bar = 200 μ m (applies to all 3 panels). (B) Corresponding manual counting of Fos-positive (+) nuclei in the arcuate nucleus in adult mice ($n = 10-12$ /group). (C) Ghrelin-induced 90-min food intake (in g/kg body weight, bw) in adult mice prior to perfusion ($n = 10-12$ /group). Symbols indicate significant differences: vs. the saline condition at * $p < 0.05$, ** $p \leq 0.01$ or † $0.05 \leq p < 0.1$; vs. the homozygous littermates under ghrelin condition at ## $p \leq 0.01$.

$p = 0.001$; and 24 h, $p = 0.005$) and heterozygous mice (3 h, $p = 0.009$; and 24 h, $p = 0.007$), but this orexigenic effect was not significant in the homozygous littermates (3 h, $p = 0.455$; and 24 h, $p = 0.329$) (Figure 3A and B).

Following the same trend, ghrelin administration, unlike saline, caused a drastic transient weight gain (Treatment: $F_{(1,23)} = 23.657$, $p < 0.001$; Time \times Genotype: $F_{(2,23)} = 2.673$, $p = 0.092$), that was obvious in wild-type ($p = 0.006$) and heterozygous mice ($p = 0.003$), but again not in homozygous mice ($p = 0.406$) (Figure 3C).

Consistent with the food intake data, peripheral ghrelin activated cells in the Arc (Treatment: $F_{(1,32)} = 5.213$, $p = 0.031$; Treatment \times Genotype: $F_{(2,32)} = 3.312$, $p = 0.052$), as assessed by the detection of the number of cells expressing Fos-like immunoreactivity, similarly in wild-type ($p = 0.033$) and heterozygous mice ($p = 0.024$), but not in homozygous mice ($p = 0.496$) (Figure 4A, B). Because the mice were perfused 90 min post-ghrelin administration, we had the opportunity to confirm our previous results on food intake by measuring it again within that period. Ghrelin-induced food intake did indeed differ among genotypes (Treatment: $F_{(1,32)} = 15.831$, $p < 0.001$; Treatment \times Genotype: $F_{(2,32)} = 2.562$, $p = 0.096$), being significant in wild-type mice ($p = 0.005$) although it did not reach statistical significance in heterozygous mice ($p = 0.072$) (Figure 4C).

3.3. Although lighter, homozygous *Ghnr-IRES-Cre* mice do not display an aberrant physical or motor development compared to their littermates

In view of our surprising result indicating that homozygous mutants are lighter than their wild-type and heterozygous littermates in adulthood, we performed another study in search of any potential physical and/or motor deficiency that could be underlying a blunted body weight. To that end, we followed pups from the three genotypes from PND 12 until adulthood.

First and foremost, breeding of heterozygous *Ghnr-IRES-Cre* pairs produced normal size litters (7 different litters assessed, consisting in average of 8.28 ± 0.75 pups) of phenotypically normal pups that were born following the expected Mendelian frequency for genotype and sex, and were indistinguishable across genotypes at birth. Importantly, 12- to 16-day-old mice performed the tail pull reflex test, as well as the cling and climb tasks equivalently regardless of genotype (Figure 5A), thereby suggesting that motor function was not compromised in homozygous pups. Likewise, horizontal activity, locomotion, and rearing activity did not differ between littermates when assessed during mid-adolescence in an open field (Figure 5B). Regarding physical development, the eye-opening test revealed no delayed maturation in homozygous mice (Figure 5A).

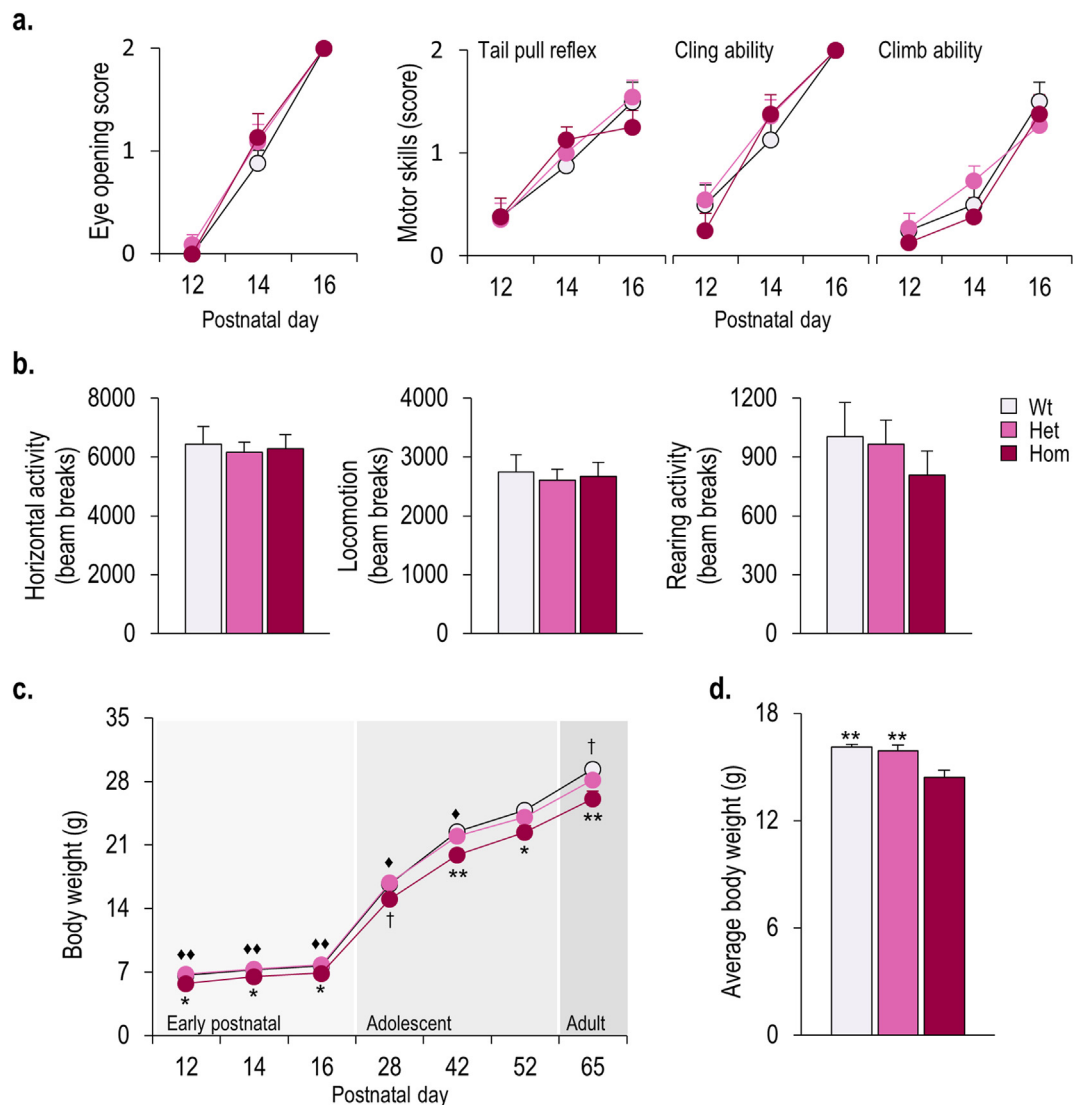


Figure 5: Physical and motor milestones in early postnatal wild-type, heterozygous and homozygous *Ghnr-IRES-Cre* mice. (A) Eye opening score and motor skills (tail pull reflex, cling, and climb abilities) tested in 12 to 16-day-old littermates ($n = 8-11/\text{group}$). (B) General locomotor activity assessed in an open field (horizontal activity, locomotion, and rearing activity) in 42-day-old littermates ($n = 8-11/\text{group}$). (C) Body weight development in early postnatal, adolescent, and adult littermates ($n = 8-11/\text{group}$), together with average body weight for the entire testing period. Symbols indicate significant differences: vs. wild-types and homozygotes at $*p < 0.05$, $**p \leq 0.01$ or $\dagger 0.05 \leq p < 0.1$ (panel c); vs. heterozygotes and homozygotes at $\blacklozenge p < 0.05$, $\blacklozenge\blacklozenge p \leq 0.01$ or $\dagger 0.05 \leq p < 0.1$ (panel C); vs. the homozygous littermates at $**p \leq 0.01$ (panel D).

Although littermates were similar in appearance at birth, their body weight progression differed from that of PND 12 (Genotype: $F_{(2,26)} = 7.970$, $p = 0.002$) (Figure 5C). Surprisingly, homozygous mice displayed already a lower body weight than their wild-type and heterozygous littermates at PND 12 ($p = 0.017$ and $p = 0.003$, respectively). Thereafter, these genotype-dependent differences remained significant throughout the early postnatal period (homozygous vs. wild-type and/or heterozygous, PND 14: $p = 0.018$ and $p = 0.005$; PND 16: $p = 0.034$ and $p = 0.004$), adolescence (PND 28: $p = 0.058$ and $p = 0.020$; PND 42: $p = 0.007$ and $p = 0.020$; PND 52: $p = 0.017$) and adulthood (PND 65: $p = 0.007$ and $p = 0.070$), such that homozygous mice weighed in average 10% less than their counterparts (average body weight between the ages of 12–65) (Figure 5D).

3.4. Adult homozygous *Ghnr-IRES-Cre* mice develop reduced body length together with lower fat mass and altered bone parameters

In concomitance with a reduced body weight, homozygous mice were also 3.5% and 2.1% shorter than wild-type ($p = 0.001$) and heterozygous littermates ($p = 0.050$), respectively, by the completion of the study (Genotype: $F_{(2,26)} = 8.293$, $p = 0.002$) (Table 2).

To elucidate the underlying causes for this somewhat unexpected effect on body weight, we explored body composition at PND 65 by means of a DXA scan. Interestingly, homozygous mice had 33% less fat mass than wild-type peers (Genotype: $F_{(2,26)} = 5.066$, $p = 0.015$; $p = 0.011$), although any differences in leptin levels (that reflect fat mass) did not reach statistical significance (Table 2). Accordingly, they also exhibited 14% and 10% less soft tissue mass compared to wild-type ($p = 0.002$) and heterozygous littermates ($p = 0.024$), respectively (Genotype:

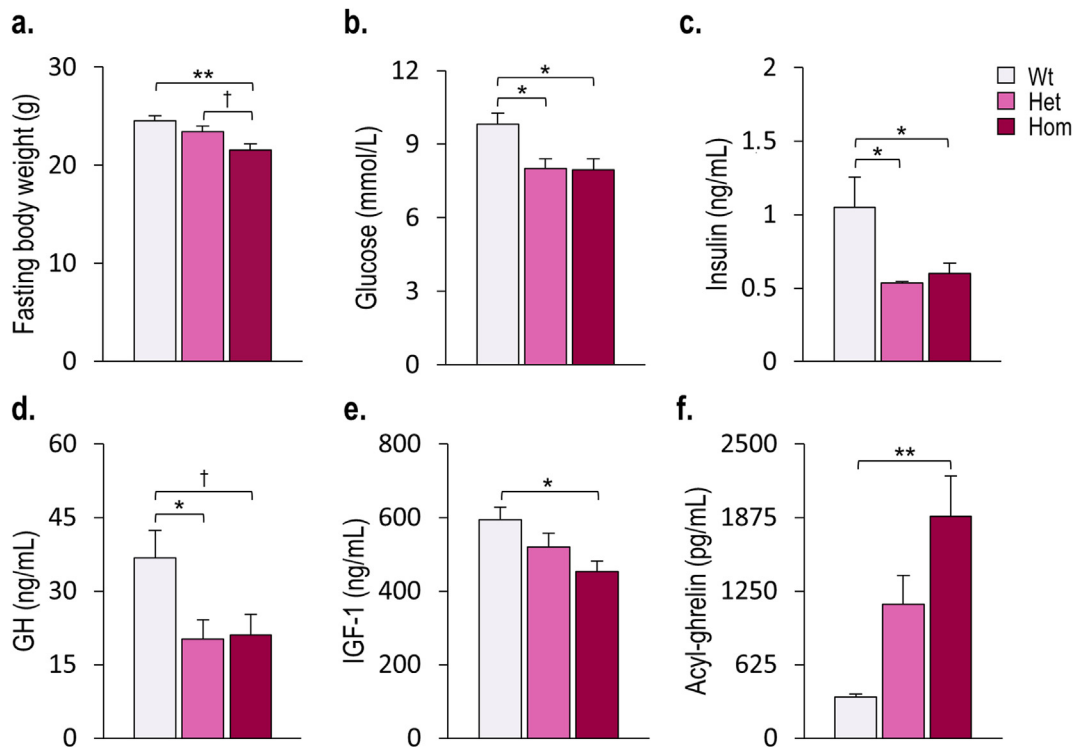


Figure 6: Metabolic effects upon an overnight fast in adult wild-type, heterozygous and homozygous *Ghnr-IRES-Cre* mice. (A) Fasting body weights (n = 8–11/group), (B) blood glucose (n = 7–11/group), (C) serum insulin levels (n = 8/group), (D) serum growth hormone (GH; n = 8–11/group), (E) serum insulin-like growth factor-1 (IGF-1; n = 8–11/group), and (F) serum acyl-ghrelin (n = 7–11/group) in 66-day-old littermates. * $p < 0.05$, ** $p \leq 0.01$ or † $0.05 \leq p < 0.1$.

Table 2 — Body composition and physical endpoints in adult (PND 65 or 66) *Ghnr-IRES-Cre* wild-type, heterozygous, and homozygous littermates.

Endpoint	Wild-type	Heterozygous	Homozygous
Body length (mm)	87.83 ± 0.51**	86.50 ± 0.43*	84.72 ± 0.62
Femur length (mm)	15.51 ± 0.08	15.44 ± 0.07	15.29 ± 0.12
Soft tissue mass (g)	28.70 ± 0.58**	27.54 ± 0.51*	24.97 ± 0.88
Lean tissue mass (g)	21.41 ± 0.60	21.30 ± 0.49	20.35 ± 0.83
Fat tissue mass (g)	7.29 ± 0.55*	6.24 ± 0.42	5.23 ± 0.26
BMI (g/cm ²)	0.381 ± 0.006	0.377 ± 0.005	0.364 ± 0.009
Leptin levels (ng/mL)	2.87 ± 1.17	2.20 ± 0.64	1.04 ± 0.22
Bone area (cm ²)	8.89 ± 0.08*	8.79 ± 0.13†	8.46 ± 0.08
Bone mineral content (mg)	707.17 ± 8.90*	687.84 ± 14.67	652.70 ± 15.19
Bone mineral density (mg/cm ²)	79.55 ± 0.90	78.22 ± 1.09	77.09 ± 1.20

The symbols indicate differences vs. the homozygous littermates at * $p < 0.05$, ** $p \leq 0.01$ or † $0.05 \leq p < 0.1$.

$F_{(2,26)} = 7.695$, $p = 0.003$) (Table 2). Strikingly, different bone parameters were also significantly affected in homozygous mice (Genotype: Bone area, $F_{(2,26)} = 3.839$, $p = 0.036$; BMC, $F_{(2,26)} = 3.529$, $p = 0.043$). In particular, homozygous mice had a decreased bone area compared to wild-type ($p = 0.038$) and heterozygous peers ($p = 0.098$), and a lower BMC than that of wild-types ($p = 0.037$). The genotype, however, did not cause lean mass, BMI or BMD to differ.

3.5. Both heterozygous and homozygous *Ghnr-IRES-Cre* mice exhibit a markedly blunted GH response together with an exaggerated drop in blood glucose and insulin upon fasting
All the mice were then subjected to an overnight fast, with a view to increasing endogenous ghrelin levels, enabling us to explore whether

the genotype affected both the glucoregulatory and the GH-releasing actions of the hormone under physiological conditions.

Genotype-dependent differences in body weight were still evident after fasting (Genotype: $F_{(2,26)} = 6.025$, $p = 0.008$): homozygous mice continued to be lighter than their wild-type ($p = 0.006$) and heterozygous littermates ($p = 0.081$) (Figure 6A). Strikingly, a steeper decrease in blood glucose was noted, not only for homozygous mice ($p = 0.022$), but also for the heterozygous littermates ($p = 0.017$), compared to wild-type controls (Genotype: $F_{(2,25)} = 5.508$, $p = 0.011$) (Figure 6B). Accordingly, both homozygous ($p = 0.046$) and heterozygous mice ($p = 0.020$) exhibited lower insulin levels than wild-types (Genotype: $F_{(2,23)} = 5.126$, $p = 0.015$) (Figure 6C). Similarly, serum GH only increased in response to fasting in wild-type mice (Genotype: $F_{(2,26)} = 3.996$, $p = 0.011$; wild-type vs. homozygous, $p = 0.073$; wild-type vs. heterozygous, $p = 0.039$) (Figure 6D). Conceivably, coinciding with the decreased body weight and body length observed in homozygous mice, serum levels of IGF-1, a hormone released by GH, were lower than those of wild-type mice (Genotype: $F_{(2,26)} = 3.492$, $p = 0.047$; wild-type vs. homozygous, $p = 0.037$) (Figure 6E). Unexpectedly, serum acyl-ghrelin levels increased in a genotype-dependent manner (Genotype: $F_{(2,25)} = 7.671$, $p = 0.003$), but this effect was only significant for homozygous vs. wild-type mice ($p = 0.002$) (Figure 6F).

4. DISCUSSION

Herein we provide evidence that inserting an *IRES-Cre* cassette into the 3'-UTR of the murine *Ghnr* gene markedly interferes with GHSR expression, as indicated by the gene-dosage deletion of GHSR in the hypothalamic Arc, one of the otherwise richest GHSR-expressing sites

in the brain. Despite showing fewer *Ghsr*-expressing cells compared to wild-types, heterozygous mice, unlike homozygous peers, remained responsive to administered ghrelin and appeared to be phenotypically normal. Conversely, homozygous mice were unresponsive to administered ghrelin and also developed a growth phenotype: they were not only lighter than their littermates, but also shorter, had less fat tissue content and altered bone parameters, and exhibited lower IGF-1 levels. Furthermore, both heterozygotes and homozygotes showed an altered endocrine response to fasting, indicative of impaired GHSR-signalling in both genotypes. In particular, and most notably, the impact of fasting on GH release and glucose homeostasis was altered even when the functionality of only one copy of the *Ghsr* gene was inadvertently reduced by the inserted *IRES-Cre* cassette.

In the present study, we unexpectedly found that endogenous *Ghsr* expression was dose-dependently disrupted in *Ghsr-IRES-Cre* mice, with the homozygous mutants being the most affected. Consistently, homozygotes did not respond to exogenous ghrelin, as indicated by their failure to acutely increase food intake and body weight or show increased Fos expression in the Arc upon peripheral ghrelin administration. These results match those previously reported in GHSR knockout (KO) and GHSR-null mice by others [18,19,21] and, besides further confirming that the orexigenic activity of ghrelin is exclusively mediated through the GHSR, they attest that homozygous *Ghsr-IRES-Cre* mice share common traits with other validated models of suppressed GHSR signalling. Importantly, the lack of significant changes in basal food intake between genotypes further support the idea that ghrelin is not indispensable for sustaining spontaneous food intake, and hence may not be an essential orexigenic factor [19].

In the study of Mani et al. (2017), heterozygous *Ghsr-IRES-Cre* mice were subjected to stereotaxic deliveries of viral vectors into the MBH to explore: (i) the effects of administered ghrelin and an overnight fast on food intake using an inhibitory designer receptor exclusively activated by designer drugs (DREADD); and (ii) the impact on baseline food intake using an excitatory DREADD [12]. Our data are in accordance with their finding that heterozygous *Ghsr-IRES-Cre* mice remain orexigenically responsive to administered ghrelin, and further suggest that the notable difference in the number of *Ghsr*-positive cells we observed between heterozygotes and wild-type controls might not be of critical relevance to preserve responsiveness to administered ghrelin. We therefore infer that heterozygous *Ghsr-IRES-Cre* mice but not homozygous mutants, can still be a useful tool in conjunction with administered ghrelin, such as when studying ghrelin-induced orexigenic effects. However, we also found that the usual GH secretory and blood glucose responses to an overnight fast were blunted to the same degree in heterozygous *Ghsr-IRES-Cre* mice as in homozygous *Ghsr-IRES-Cre* mice, suggesting that partial reductions in *Ghsr* expression can substantively affect certain aspects of physiology related to GHSR signalling.

Our assertion here that inserting the *IRES-Cre* cassette into the endogenous *Ghsr* locus does indeed interfere with GHSR signalling in the *Ghsr-IRES-Cre* model is also supported by our observation that homozygous mice exhibited lower body weights compared to their littermates, a phenotype that has been previously reported to occur, albeit not without some disagreements, in other mouse models of altered GHSR signalling [15–21,34]. Some of the initial targeted-deletion studies found either insignificant [18] or mere slight differences in body weight and/or adiposity between littermates, either under regular chow or upon a high-fat diet challenge [19,20]. On the contrary, other studies have reported that GHSR KO mice and GHSR-null mice, especially at older ages, are remarkably lighter (in particular, due to a lower body fat content) than wild-type controls

[15,16,21]. Although littermates were physically indistinguishable across genotypes at birth, we did not explicitly monitor their body weight at such early life stage, but only from PND 12; it may be that the homozygous mutants were already born with the lowest body weight. That said, a previous study comparing male GHSR-null mice vs. wild-type littermate controls prior to weaning at PND 28 demonstrated overlapping body weights on PND 0 and a subsequent divergence of body weight curves at just about PND 12 [35]. To rule out any potential congenital abnormality that could be concealing the body weight phenotype, we tested motor and physical abilities during the early postnatal period. Notably, we did not find the genotype to influence developmental motor milestones or locomotor activity in an OF, thus dismissing the possibility that neither physical nor motor impairments contributed to or underlie the leaner phenotype. Conversely, it has been shown that the 129/SvEvTac mouse strain, from which the embryonic stem cells used to create transgenic mouse models such as that used in this study are derived, favours a lean phenotype [36]. However, we backcrossed the *Ghsr-IRES-Cre* transgenic colony for far greater than six generations to C57BL/6N, which should have ensured an evenly distributed genetic background among littermates. The general absence of a growth phenotype (that would, at least in part, account for a body weight phenotype) in mice lacking components of the ghrelin system has remained perplexing, given the well-established role of ghrelin as a GH secretagogue. Supporting the development of reduced body weight in homozygous *Ghsr-IRES-Cre* mice, the latter were also 3.5 and 2.1% shorter (nose-to-anus length) than wild-type and heterozygous littermates, respectively. Likely reminiscent of the decreased body length, total bone area, as well as BMC were likewise decreased in homozygous mice, while serum GH and IGF-1 (a downstream GH effector) levels were also reduced in overnight-fasted homozygous mutants. Collectively, these data point to a growth impairment together with a pattern of defective GH secretion resulting from an absent GHSR signalling in the homozygous mutants, and thus underscore an alteration in the GH-growth axis in these mice. These observations have been also partially reported in mice lacking either GHSR or both ghrelin and GHSR, which appeared to be shorter than wild-type mice, yet serum levels of IGF-1 remained similar between genotypes [17,21]. Interestingly, 15 years ago, Pantel and colleagues identified a naturally occurring GHSR mutation that impairs GHSR constitutive activity [37]. This GHSR mutation that replaces alanine at position 204 with glutamate (GHSR-A204E) is associated with a high penetrance of short stature, which might be assumed to result from impaired GH secretion due to the mutant GHSR [37]. More recently, a mouse model (GHSR-A203E) of that human mutation [34] was shown to be lighter than wild-type littermates and to exhibit decreased body length and defective GH secretion in response to a severe caloric restriction protocol.

Perhaps one of the most striking results of the present study relates to the metabolic response of heterozygous *Ghsr-IRES-Cre* mice upon an overnight fast. Indeed, although both the RNAscope data and the acute studies with administered ghrelin made us somewhat anticipate the metabolic response in overnight-fasted homozygotes, we were surprised by the fact that heterozygous mice shared most of the traits with their homozygous peers. Arguably, under fasting conditions, endogenous ghrelin levels would trigger an elevation in plasma GH, at least in mice with intact GHSR functioning, which would eventually be engaged in preventing the development of fasting-induced severe hypoglycaemia. Expectedly, the homozygotes did not show any substantial increase in GH release upon an overnight fast, as it was the case for other mouse models of reduced or absent GHSR signalling [19,34,38]. Consistently, the absence of GH would have caused both glucose and

insulin levels to drop, as observed previously in GHSR-KO mice [21]. Interestingly, heterozygous mice also displayed lower GH, glucose, and insulin levels (compared to wild-type controls). Collectively these data suggest that harbouring one copy of the *IRES-Cre* cassette alone is enough to generate (at least metabolically) a GHSR-null phenotype. Besides a lower amount of *Ghsr* transcript levels (compared to wild-types), there are other several possible explanations for this unexpected result. Presumably, it might be that inserting a *Cre* sequence into the *Ghsr* gene impacted *per se* the inherent genome machinery, thus affecting the correct functioning of the cell itself. Although it would have been interesting to empirically evaluate whether the targeted cells are critically affected by this genetic manipulation, the potential toxicity may have led cells to death, fact that would have eventually hindered their detection. In any case, Mani and colleagues demonstrated that heterozygous *Ghsr-IRES-Cre* mice injected with excitatory DREADDs into the MBH increased baseline food intake [12], thereby implying that the transgene does not negatively impact the orexigenic capacity of GHSR-expressing MBH neurons and thus that expression of *Cre per se* does not affect general cell function. On the other hand, the dose of ghrelin we used for the acute studies (3 mg/kg body weight; [39]) was likely too high to mimic endogenous ghrelin levels upon fasting. Thus, it might be that under non-physiological conditions, exogenous circulating ghrelin recruited all the available GHSR in heterozygous mice to a threshold, fact that would explain both the increased acute feeding response and Fos protein expression in the Arc. However, under physiological fasting conditions, ghrelin levels would be arguably much lower and, in conjunction with diminished GHSR, they might not have been sufficient to successfully trigger neither GH release nor the correlated increases in glucose and insulin levels in heterozygous mutants. Yet another possibility is that in addition to the gene-dosage effect of reduced *Ghsr* expression, cell toxicity potentially related to a gene-dosage effect of *Cre* expression within all GHSR-expressing cells could be contributing to the observed metabolic phenotypes.

To our knowledge, the *Ghsr-IRES-Cre* mouse model (especially the homozygous mutants) is the first model of decreased GHSR signalling in which fasting levels of acyl-ghrelin have been shown to be increased. This resonates with an interrupted feedback loop in which ghrelin-sensing is disrupted such that the stomach releases more acyl-ghrelin. The level at which this feedback inhibition occurs is unclear. Interestingly, it could be due to reduced GH feedback inhibition of ghrelin release [40] since serum GH levels were reduced according to a gene-dose effect. Conversely, heightened ghrelin levels during fasting may represent a failed attempt to restore body weight and/or body growth in these homozygous mice that have a short/lean phenotype. Recently, the Kaplan lab [41] discovered a new endogenous GHSR antagonist, namely liver-expressed antimicrobial peptide-2 (LEAP-2), which has been reported to fully inhibit GHSR activation by ghrelin and to block the major effects of ghrelin *in vivo*. In their seminal work, the authors suggested that LEAP-2 may present a dual mechanism of inhibiting ghrelin action, both by antagonizing the GHSR and by inhibiting ghrelin production [41]. Given the potential of this peptide in the treatment of obesity and other diseases that involve dysregulation of the ghrelin system [42], it would be interesting to evaluate the action of LEAP-2 in an animal model of suppressed GHSR signalling, such as the *Ghsr-IRES-Cre* homozygous mice herein presented; these studies might help to determine whether the regulation of ghrelin production by LEAP-2 occurs through GHSR antagonism or a distinct mechanism. It is worth emphasizing that the novel *Ghsr-IRES-Cre* mouse model was generated using methods that minimise interference with native protein expression. Indeed, the transgene was knocked-in, by

homologous recombination, into a non-coding region, 3 base pairs after the *Ghsr* STOP codon (i.e., 3'-UTR) [12], and thus does not excise or replace any coding part of the endogenous *Ghsr* gene. Moreover, the presence of an *IRES* sequence theoretically prevents expression of the *Ghsr* gene; it ensures that both *Ghsr* and *Cre* genes are co-expressed under the control of the *Ghsr* promoter, eventually resulting in two independent proteins. Although we did not explicitly assess Arc *Cre* expression in this study, both *Cre* and *Ghsr* transcript levels would be expected to follow the same allele-dependent trend, because both genes are transcribed into the same mRNA: the IRES sequence takes action during translation, and not transcription. In spite of these circumventing methods, our results herein resonate with previous studies demonstrating that, even when inserted into the 3'-UTR, the transgene can unwittingly interfere with the expression of the targeted gene even in the most well-constructed models [24–27]. Several studies have highlighted a role of the highly-conserved 5' and 3'-UTRs of mRNAs in regulating mRNA function [43]. For example, UTRs can affect mRNA nuclear export, cytoplasmic localisation, translational efficiency, and stability. However, any reason as to why *Ghsr* expression would be dose-dependently reduced in mutant mice remains speculative and thus deserves to be further investigated.

Although the development of transgenic *Cre*-based driver lines has undeniably revolutionised neuroscience, very few techniques come without pitfalls. Recognizing and exploring such constraints prior to drawing any physical or physiological conclusion is key to ensure a correct interpretation of the valuable data these transgenic lines may generate. From the present study, we conclude that inserting an *IRES-Cre* cassette into the 3'UTR of the *Ghsr* gene allele-dependently blunts endogenous *Ghsr* expression in the Arc. Consequently, homozygous mutants display a pronounced phenotype of defective GHSR signalling, including a growth-retarded profile. Thence, we propose that these mice, which have more pronounced signs of GHSR lack-of-function than any other mouse strain of suppressed GHSR signalling described to date, could be regarded as a new model of GHSR knock down. Importantly, because we detected metabolic signs of GH dysfunction not only in homozygous mutants, but also in heterozygous *Ghsr-IRES-Cre* mice, these data most probably conceal additional subtle effects (for the phenotype emerging) upon insertion of a single copy of the *IRES-Cre* transgene. Therefore, such limitations should be considered for further studies using this specific and other *Cre* transgenic mouse lines.

AUTHOR CONTRIBUTIONS

Conceptualisation, FP-S, SLD, RAHA and JMZ; Study design, FP-S and IS; Investigation, FP-S, IS and MVL; Formal analysis, FP-S; Visualisation, FP-S; Writing — Original Draft, FP-S; Writing — Review & Editing, all authors; Funding acquisition, SLD; Resources, JMZ. All authors approved the manuscript for publication.

ACKNOWLEDGEMENTS

This study was supported by the Swedish Research Council (Vetenskapsrådet, 2018-02588 to RAHA and 2019-01051 to SLD), Hjärfonden (F02017-0180, F02018-0262, F02019-0086 to SLD), the Novo Nordisk Fonden (NNF170C0027206 and NNF190C0056694 to SLD), Avtal om Läkarutbildning och Forskning (ALFGBG-723681 to SLD) and the NIH (R01DK119341-01A1 and P01DK119130-01A1 to JMZ). We thank Prof. Zane B Andrews for providing a breeding pair of *Ghsr-IRES-Cre* for use in this study, Prof. Claes Ohlsson for lending us the DXA chamber, Prof. John-Olov Jansson and Dr. Erik Schéle for valuable insights, Dr. Romana Stark for sharing with us her genotyping protocol, and Dr. Ulrika Bergström for fine-tuning it. We

acknowledge the Centre for Cellular Imaging at the University of Gothenburg and the National Microscopy Infrastructure, NMI (VR-RFI 2016-00968) for providing access to their confocal microscope and for their assistance. We also thank ECNP for shared expertise via the Nutrition network.

CONFLICT OF INTEREST

None declared.

REFERENCES

- [1] Cummings, D.E., Frayo, R.S., Marmonier, C., Aubert, R., Chapelot, D., 2004. Plasma ghrelin levels and hunger scores in humans initiating meals voluntarily without time- and food-related cues. *American Journal of Physiology. Endocrinology and Metabolism* 287(2):E297–E304.
- [2] Cummings, D.E., Purnell, J.Q., Frayo, R.S., Schmidova, K., Wisse, B.E., Weigle, D.S., 2001. A preprandial rise in plasma ghrelin levels suggests a role in meal initiation in humans. *Diabetes* 50(8):1714–1719.
- [3] Kojima, M., Hosoda, H., Date, Y., Nakazato, M., Matsuo, H., Kangawa, K., 1999. Ghrelin is a growth-hormone-releasing acylated peptide from stomach. *Nature* 402(6762):656–660.
- [4] Wren, A.M., Seal, L.J., Cohen, M.A., Brynes, A.E., Frost, G.S., Murphy, K.G., et al., 2001. Ghrelin enhances appetite and increases food intake in humans. *The Journal of Clinical Endocrinology & Metabolism* 86(12):5992.
- [5] Wren, A.M., Small, C.J., Abbott, C.R., Dhillo, W.S., Seal, L.J., Cohen, M.A., et al., 2001. Ghrelin causes hyperphagia and obesity in rats. *Diabetes* 50(11):2540–2547.
- [6] Mani, B.K., Uchida, A., Lee, Y., Osborne-Lawrence, S., Charron, M.J., Unger, R.H., et al., 2017. Hypoglycemic effect of combined ghrelin and glucagon receptor blockade. *Diabetes* 66(7):1847–1857.
- [7] Tschöp, M., Smiley, D.L., Heiman, M.L., 2000. Ghrelin induces adiposity in rodents. *Nature* 407(6806):908–913.
- [8] Bake, T., Edvardsson, C.E., Cummings, C.J., Dickson, S.L., 2019. Ghrelin's effects on food motivation in rats are not limited to palatable foods. *Journal of Neuroendocrinology* 31(7):e12665.
- [9] Cornejo, M.P., Barrile, F., De Francesco, P.N., Portiansky, E.L., Reynaldo, M., Perello, M., 2018. Ghrelin recruits specific subsets of dopamine and GABA neurons of different ventral tegmental area sub-nuclei. *Neuroscience* 392:107–120.
- [10] Egecioglu, E., Jerlhag, E., Salomé, N., Skibicka, K.P., Haage, D., Bohlooly, Y.M., et al., 2010. Ghrelin increases intake of rewarding food in rodents. *Addiction Biology* 15(3):304–311.
- [11] Walker, A.K., Ibia, I.E., Zigman, J.M., 2012. Disruption of cue-potentiated feeding in mice with blocked ghrelin signaling. *Physiology & Behavior* 108:34–43.
- [12] Mani, B.K., Osborne-Lawrence, S., Mequinion, M., Lawrence, S., Gautron, L., Andrews, Z.B., et al., 2017. The role of ghrelin-responsive mediobasal hypothalamic neurons in mediating feeding responses to fasting. *Molecular Metabolism* 6(8):882–896.
- [13] Mani, B.K., Walker, A.K., Lopez Soto, E.J., Raingo, J., Lee, C.E., Perelló, M., et al., 2014. Neuroanatomical characterization of a growth hormone secretagogue receptor-green fluorescent protein reporter mouse. *Journal of Comparative Neurology* 522(16):3644–3666.
- [14] Zigman, J.M., Jones, J.E., Lee, C.E., Saper, C.B., Elmquist, J.K., 2006. Expression of ghrelin receptor mRNA in the rat and the mouse brain. *Journal of Comparative Neurology* 494(3):528–548.
- [15] Ma, X., Lin, L., Qin, G., Lu, X., Fiorotto, M., Dixit, V.D., et al., 2011. Ablations of ghrelin and ghrelin receptor exhibit differential metabolic phenotypes and thermogenic capacity during aging. *PLoS One* 6(1):e16391.
- [16] Lin, L., Saha, P.K., Ma, X., Henshaw, I.O., Shao, L., Chang, B.H., et al., 2011. Ablation of ghrelin receptor reduces adiposity and improves insulin sensitivity during aging by regulating fat metabolism in white and brown adipose tissues. *Aging Cell* 10(6):996–1010.
- [17] Pfluger, P.T., Kirchner, H., Günzel, S., Schrott, B., Perez-Tilve, D., Fu, S., et al., 2008. Simultaneous deletion of ghrelin and its receptor increases motor activity and energy expenditure. *American Journal of Physiology — Gastrointestinal and Liver Physiology* 294(3):G610–G618.
- [18] Sun, Y., Ahmed, S., Smith, R.G., 2003. Deletion of ghrelin impairs neither growth nor appetite. *Molecular and Cellular Biology* 23(22):7973–7981.
- [19] Sun, Y., Wang, P., Zheng, H., Smith, R.G., 2004. Ghrelin stimulation of growth hormone release and appetite is mediated through the growth hormone secretagogue receptor. *Proceedings of the National Academy of Sciences of the United States of America* 101(13):4679–4684.
- [20] Wortley, K.E., Anderson, K.D., Garcia, K., Murray, J.D., Malinova, L., Liu, R., et al., 2004. Genetic deletion of ghrelin does not decrease food intake but influences metabolic fuel preference. *Proceedings of the National Academy of Sciences of the United States of America* 101(21):8227–8232.
- [21] Zigman, J.M., Nakano, Y., Coppari, R., Balthasar, N., Marcus, J.N., Lee, C.E., et al., 2005. Mice lacking ghrelin receptors resist the development of diet-induced obesity. *Journal of Clinical Investigation* 115(12):3564–3572.
- [22] Sternberg, N., 1981. Bacteriophage P1 site-specific recombination. III. Strand exchange during recombination at lox sites. *Journal of Molecular Biology* 150(4):603–608.
- [23] Wang, X., 2009. Cre transgenic mouse lines. *Methods in Molecular Biology* 561:265–273.
- [24] Bäckman, C.M., Malik, N., Zhang, Y., Shan, L., Grinberg, A., Hoffer, B.J., et al., 2006. Characterization of a mouse strain expressing Cre recombinase from the 3' untranslated region of the dopamine transporter locus. *Genesis* 44(8):383–390.
- [25] Joye, D.A.M., Rohr, K.E., Keller, D., Inda, T., Telega, A., Pancholi, H., et al., 2020. Reduced VIP expression affects circadian clock function in VIP-IRES-CRE mice (JAX 010908). *Journal of Biological Rhythms* 35(4):340–352.
- [26] Rashid, H., Chen, H., Hassan, Q., Javed, A., 2017. Dwarfism in homozygous *Aqc1*(CreERT) mice is associated with decreased expression of aggrecan. *Genesis* 55(10).
- [27] Viollet, C., Simon, A., Tolle, V., Labarthe, A., Grouselle, D., Loe-Mie, Y., et al., 2017. Somatostatin-IRES-Cre mice: between knockout and wild-type? *Frontiers in Endocrinology* 8:131.
- [28] Le May, M.V., Peris-Sampedro, F., Stoltenborg, I., Schéle, E., Bake, T., Adan, R.A.H., et al., 2021. Functional and neurochemical identification of ghrelin receptor (GHSR)-expressing cells of the lateral parabrachial nucleus in mice. *Frontiers in Neuroscience* 15(132).
- [29] de Vrind, V.A.J., Rozeboom, A., Wolterink-Donselaar, I.G., Lujendijk-Berg, M.C.M., Adan, R.A.H., 2019. Effects of GABA and leptin receptor-expressing neurons in the lateral hypothalamus on feeding, locomotion, and thermogenesis. *Obesity* 27(7):1123–1132.
- [30] Le May, M.V., Hume, C., Sabatier, N., Schéle, E., Bake, T., Bergström, U., et al., 2019. Activation of the rat hypothalamic supramammillary nucleus by food anticipation, food restriction or ghrelin administration. *Journal of Neuroendocrinology* 31(7):e12676.
- [31] Basaure, P., Guardia-Escote, L., Cabré, M., Peris-Sampedro, F., Sánchez-Santed, F., Domingo, J.L., et al., 2018. Postnatal chlorpyrifos exposure and apolipoprotein E (APOE) genotype differentially affect cholinergic expression and developmental parameters in transgenic mice. *Food and Chemical Toxicology* 118:42–52.
- [32] Reverte, I., Domingo, J.L., Colomina, M.T., 2014. Neurodevelopmental effects of decabromodiphenyl ether (BDE-209) in APOE transgenic mice. *Neurotoxicology and Teratology* 46:10–17.
- [33] Blatnik, M., Soderstrom, C.I., 2011. A practical guide for the stabilization of acylghrelin in human blood collections. *Clinical Endocrinology* 74(3):325–331.
- [34] Torz, L.J., Osborne-Lawrence, S., Rodriguez, J., He, Z., Cornejo, M.P., Mustafá, E.R., et al., 2020. Metabolic insights from a GHSR-A203E mutant mouse model. *Molecular Metabolism* 39:101004.

- [35] Rodriguez, J.A., Bruggeman, E.C., Mani, B.K., Osborne-Lawrence, S., Lord, C.C., Roseman, H.F., et al., 2018. Ghrelin receptor agonist rescues excess neonatal mortality in a Prader-Willi syndrome mouse model. *Endocrinology* 159(12):4006–4022.
- [36] Sun, Y., Butte, N.F., Garcia, J.M., Smith, R.G., 2008. Characterization of adult ghrelin and ghrelin receptor knockout mice under positive and negative energy balance. *Endocrinology* 149(2):843–850.
- [37] Pantel, J., Legendre, M., Cabrol, S., Hilal, L., Hajaji, Y., Morisset, S., et al., 2006. Loss of constitutive activity of the growth hormone secretagogue receptor in familial short stature. *Journal of Clinical Investigation* 116(3):760–768.
- [38] Shankar, K., Gupta, D., Mani, B.K., Findley, B.G., Lord, C.C., Osborne-Lawrence, S., et al., 2020. Acyl-ghrelin is permissive for the normal counter-regulatory response to insulin-induced hypoglycemia. *Diabetes* 69(2):228–237.
- [39] Jensen, M., Ratner, C., Rudenko, O., Christiansen, S.H., Skov, L.J., Hundahl, C., et al., 2016. Anxiolytic-like effects of increased ghrelin receptor signaling in the amygdala. *International Journal of Neuropsychopharmacology* 19(5).
- [40] Qi, X., Reed, J., Englander, E.W., Chandrashekar, V., Bartke, A., Greeley Jr., G.H., 2003. Evidence that growth hormone exerts a feedback effect on stomach ghrelin production and secretion. *Experimental Biology and Medicine* 228(9):1028–1032.
- [41] Ge, X., Yang, H., Bednarek, M.A., Gallon-Tilleman, H., Chen, P., Chen, M., 2018. LEAP2 is an endogenous antagonist of the ghrelin receptor. *Cell Metabolism* 27(2):461–469.
- [42] Al-Massadi, O., Müller, T., Tschöp, M., Diéguez, C., Nogueiras, R., 2018. Ghrelin and LEAP-2: rivals in energy metabolism. *Trends in Pharmacological Sciences* 39(8):685–694.
- [43] Hughes, T.A., 2006. Regulation of gene expression by alternative untranslated regions. *Trends in Genetics* 22(3):119–122.